arXiv:astro-ph/0602456v1 21 Feb 2006

# The dissolving Rosette HH2 jet bathed in harsh UV radiation of the Rosette Nebula

J. Z. Li[1], Y. -H. Chu[2], R. A. Gruendl[2]

[1]*National Astronomical Observatories, Chinese Academy of Sciences, 20A Datun Road, Chaoyang District, Beijing 100012, China; ljz@bao.ac.cn*

[2]*Department of Astronomy, University of Illinois, Urbana-Champaign, IL, 61801, USA*

## ABSTRACT

Herbig-Haro flows discovered in photoionized medium forms a separate category and detailed studies of which become one of the key issues to our understanding of jet production and evolution. The Rosette HH2 jet is the second of such flows that immersed in the spectacular HII region of the Rosette Nebula. However, its disconnected jet components are detached from the proposed energy source, have additional unusual properties and thus a disputable nature. In this paper, we investigate through high-quality echelle spectrographs the physical nature of the jet system. The jet shows distinctly different velocity components. It is believed to be composed of a fast neutral jet with an approaching velocity of -39.5 km $^{-1}$ as respect to the systemic rest frame, and likely an extensive, photo-evaporated envelope dissolving at roughly the sound speed. This led us to infer a fast dissipating nature of the jet system being bathed in the fully photoionized medium of Rosette.

In addition, time series photometric observations provide evidence that the energy source is highly variable, with amplitudes of up to $> 1$ mag in R & I. This is consistent well with an early evolutionary status of the jet driving star with a red, late type spectrum in the optical.

*Subject headings:* accretion disks – ISM: jets and outflows – stars: formation – stars: pre-main-sequence

## 1. Introduction

The recent discovery of an increasing number of collimated Herbig-Haro (HH) jets ejected by optically visible, young low-mass stars that immersed in HII regions makes them a separate category of HH flows (Reipurth et al. 1998; Bally et al. 2000; Bally & Reipurth

2001; Li 2003; Li & Rector 2004). Detailed investigations of these so called photoionized jets are of particular interest as they are in association with visible young stellar objects at their early stages of evolution. These jet driving sources would otherwise have been shielded by optically opaque envelopes and/or natal molecular clouds if not made visible by photoionization of the HII regions in which they reside. On the other hand, the lifetime of such photoionizing jets can be short, this makes them hard to identify and even more crucial in studies of jet production and maintenance before the beams are lost in the glare of the ionized nebulae.

Properties of the externally ionized jets are found to heavily rely on local conditions of the photoionized medium i.e. the intensity of the UV radiation field. Some jet systems such as the Rosette jets (Li 2003; Li & Rector, 2004) even contradict in properties with conventional impressions of a jet. The Rosette HH2 jet, for example, is proposed by Li (2003) as a high-excitation jet from a late type star around the central cavity of Rosette that shows an unusual appearance. It is composed of mainly two discrete knots or jet components probably in the process of photo-dissipation. These components resemble more nebulous entities, the proposed jet therefore shows an abnormally large width to length ratio which is in remarkable discrepancy from conventional impressions of a jet. Furthermore, the seemingly collimated part of the jet shows a detached appearance from both the suggested energy source and the extensive portion of the jet. This jet system displaying various anomalous features, if finally convinced, will be the only other case of a high-excitation jet that survived the harsh UV ionization of the Rosette Nebula. Numerous young stellar objects originated from the same episode of star formation in this region could have already shed their envelopes, ceased their mass ejection and the signatures of the existence of any flows were also dissipated by the external ionization. These two jet systems may well be the last two still identifiable and are also in the process of their fast photo-dissipation. Detailed studies of such jets will definitely contribute to a better understanding of the interactions between fierce external UV ionization and the jet systems, and to the final theoretical solution to jet formation and evolution and their dependence on environmental conditions. There are, however, still possibilities of solely spatial coincidence of high-excitation gas entities in Rosette along the line of sight, rather than being manifestations of discrete ejecta from the proposed energy source as a result of episodic or unsteady mass outflow? This causes confusion since its discovery and definitely awaits for further clarification by high quality observational studies. This study presents primarily the kinematics of the proposed jet system, which definitely consolidated its physical origin as a jet.

## 2. Observations and data reduction

### 2.1. Echelle Spectroscopy

Single-order echelle spectra, covering both H$\alpha$ and [NII], of the jet system were obtained with the CTIO Blanco 4m telescope and its echelle spectrograph at the Ritchey-Critchien focus on January 12, 2005. A resolving power of $\sim$ 40000 was achieved around H$\alpha$. The spectral data reduction were performed following standard procedures in IRAF. The wavelength calibration of the data has been improved by verifying the night sky lines, which is expected to be accurate to $\pm$ 1 kms$^{-1}$. The final echelle spectrogragh are corrected to the heliocentric rest frame.

### 2.2. Photometric and spectroscopic monitoring

We have initiated a simultaneous photometric and spectroscopic monitoring campaign of the jet driving sources in Rosette between Dec. 31, 2004 and Jan. 7, 2005. For a detailed description of the monitoring campaign, please refer to Section 2.3 of Li et al. (2006). Due to the faintness of the Rosette HH2 source, only two consecutive spectra were achieved by the 2.16 m telescope of the National Astronomical Observatory (NAOC) during this run of observations. The Beijing Faint Object Spectrograph and Camera (BFOSC) and a thinned back-illuminated Orbit 2k$\times$2k CCD were used. The G4 grating of BFOSC resulted in a two-pixel spectral resolution of 8.3 Å. The differential photometric observations based on the Hsing-Hua 80 cm telescope, which is located at the Xing-Long station of NAOC, were later extended to Jan. 12, 2005. Differential light variations of the jet source during this period were obtained through both the R & I band filters, resulting in differential magnitudes accurate to within 0.04 mag for both filters.

## 3. Kinematics of the jet

As mentioned in the introduction section, the proposed jet shows many unique features and its physical nature has to be clarified. The high-quality echelle spectrograph along the jet is shown by Fig. 1a. It is clear that H$\alpha$ emission from the jet is strong but has a broad appearance, which is severely blended with the background nebular emission. Fortunately, the [NII] emission lines have comparatively low dispersion in velocity and are ideally resolved from at least those from the receding shell of the HII region. Based on the well-resolved background emission in the counterjet direction, the collisionally excited [NII] emission lines

from both the approaching and the receding shells of the Nebula, indicate distinct heliocentric radial velocities ($V_{hel}$) that centered at 0.3 & 29 km s$^{-1}$, respectively. This gives a systematic expansion of 14.3 $\pm$ 1 km s$^{-1}$ of the ionized gas and a systemic $V_{hel}$ of 14.6 $\pm$ 1 km s$^{-1}$ at this part of the Rosette Nebula. It can be noteworthy that the forbidden [NII] emission from the receding side of the nebula is stronger, which hints for a larger emission measure and indicates the approaching shell is shallower than the receding part in the line of sight of the jet system.

Both the H$\alpha$ and [NII] emission from the jet, however, indicate complex structures in the velocity field. To make things clear, we present in Fig. 1b the echelle spectrograph after careful background subtraction. In general, the blue wing of the radial velocity (RV) distribution of the jet materials brakes slowly along the jet direction and finally merges with the red wing, indicating a constant RV, at the distance of the extensive part of the jet with a diffuse appearance. The is distinctively illustrated by the Position-Velocity plots shown by Figs. 2a & 2b. The RV distribution of the jet materials alone verifies that the discrete components of the jet proposed by Li (2003) are indeed kinetically and physically related.

The [NII] emission lines at $\lambda\lambda$6548 & 6583, however, are further resolved into a high-velocity component (HVC) with a heliocentric RV centered at -25 km s$^{-1}$ ($V_{sys}$=-39.5 km s$^{-1}$) and a low-velocity component (LVC) with a heliocentric RV of 5 km s$^{-1}$ ($V_{sys}$=-9.5 km s$^{-1}$) in a distinct manner. This is important as the existence of the HVC makes solid the jet nature of the system, excluding possibilities of solely evaporated clumps of gas happen to be projected in the close vicinity of the energy source, which otherwise can not reconcile with the HVC and the two fold velocity structures detected. Furthermore, the well-resolved data permit us to distinguish between the physically related outflowing components with distinct RV, which points to a clear physical picture of the jet system. It is composed of (1) a HVC that attributed to a fast neutral jet that remains propagating at the original velocity into the photoionized medium. This HVC, however, later begins to decelerate as the distance from the jet source increases due to probably external UV destruction, and (2) a LVC in association with gas entrained by the jet but keeps being photoevaporated by the strong UV field of Rosette. It shows a RV in good agreement with a fast dissipating envelope moving at the sound speed of around 10 km s$^{-1}$ (Johnstone et al. 1998). This, on the other hand, naturally explains why the jet has a large width to length ratio or why the jet components resulted from discrete mass ejection have in common an extended or even a nebular appearance, which is particular to this jet in most likely a dissolving phase. We would therefore feel safe to declare that as evidenced by both the appearance and the kinematics of the Rosette HH2 jet, we are spotting the latest stages of jet evolution or dilution in a photoionized medium.

## 4. Spectral properties of the jet system

The extracted single-order echelle spectrum of the energy source is presented by Fig. 3a, where H$\alpha$ is well resolved from the ambient [NII] emission lines. The H$\alpha$ in emission with a detected equivalent width of 6.9 Å is broad as mentioned in the above section and shows a complex profile. It has signatures of absorption in both the blue and the red wings, indicating most likely the co-existence of both mass outflow and inflow. This is in agreement with the jet driving nature of the young stellar object. The [NII] emission lines $\lambda\lambda$6548 & 6583 indicate an equivalent width of 2.1 Å and 0.4 Å, respectively. This yields a line ratio of $\sim$ 5. The extracted spectrum of the collimated part of the jet is given in Fig. 3b. Note about the broad, multi-component emission associated with its H$\alpha$ emission and the double peak profile of the forbidden [NII] emission lines, indicating the distinct existence of different velocity components in the ejected materials.

Low-resolution spectrum of the Rosette HH2 source is presented in Fig. 4, which illustrates primarily moderate H$\alpha$, prominent [OIII] emission and shows a late spectral type with a very red continuum in the optical. Low-resolution spectroscopy was employed due to the faintness of the energy source in the optical at the large distance of Rosette of 1.39 kpc (Hensberge et al. 2000). As a result, the H$\alpha$ emission is hardly resolved from the nearby [NII] emission lines. This already benefits from the comparatively low thermal width of its H$\alpha$ and nearby emission lines as compared to other active young stellar objects. The equivalent width of H$\alpha$ varies from 12.2 to 20.5 Å in the two consecutive exposures. The stronger emission from H$\alpha$ detected by the low-resolution spectroscopy is attributed to more likely the highly variable nature of the jet source rather than a significant contribution from the blended [NII] emission lines. However, its high state of excitation as revealed by the prominent [OIII] emission lines at $\lambda\lambda$4959 & 5007 strongly suggests a fully ionized origin of at least the outer layers of the relic disk in association. This will definitely result in a rapid photodissipation of the system.

## 5. Variability of the jet-driving source

Results from the photometric monitoring in R and I were presented by Figs. 5a & 5b, respectively. It is clear that both lightcurves show anomalously strong photometric variations in a largely consistent way in both bands. This convinces us the large amplitude variations are true in light of the small photometric uncertainty in each band (please refer to section 2.2). Furthermore, possibly two consecutive eruptive events with similar amplitudes of $\sim$1.4 mag in R and 1.25 mag in I, respectively, were detected by the 13 days monitoring campaign. Its large amplitude of variation is commensurate with and set solid its young status evolution

of the energy source. The erratic light variations are most likely attributed to prominent chromospheric activity or rather unsteady mass accretion from at most a relic disk (Li 2005).

## 6. Summary

Based on our high-spatial and high-spectral resolution spectroscopy by the Blanco 4m telescope of CTIO, we presented for the first time the kinematics of the Rosette HH2 jet, which clarified also its physical nature of the jet system. The collimated part of the jet shows clearly two distinct velocity components i.e. a HVC with a RV of -39.5 km $s^{-1}$ and a LVC with a RV of -9.5 km $s^{-1}$ as respect to the rest frame of Rosette. We thus conclude that the jet is composed of a neutral core that remains propagating at its original velocity into the photoionized medium, and a fast dissipating envelope dissolving at roughly the sound speed. This jet system, along with the Rosette HH1 jet, is believed to be in a process of fast dissipation due to the harsh UV radiation field in which it resides. The time series photometric observations signifies a highly variable nature of the jet driving source, in nice agreement with its young stage of evolution and possibly an association with a relic disk also in the fate of photoevaporation and dissipation.

**Acknowledgments**

Thanks to Y. L. Qiu and J. Zh. Li for coordinating the photometric observations with the Hsing-Hua 80 cm telescope. The author is grateful to W. Su for her help on the data reduction. This project is supported by the National Natural Science Foundation of China through grant O611081001.

## REFERENCES

Bally, J., O'Dell, C. R., McCaughrean, M. J., 2000, AJ 119, 2919

Bally, J. & Reipurth, B., 2001, ApJ 546, 299

Hensberge, H. Pavlovski, K. & Verschueren, W. 2000, A&A 358, 553

Johnstone, D., Hollenbach, D. & Bally, J. 1998, ApJ 499, 758

Li, J. Z. 2003, ChJAA Lett. 6, 495

Li, J. Z. 2005, ApJ 625, 242

Li, J. Z. & Rector, T. A., 2004, ApJ 600, L67

Li, J. Z., Y. -H. Chu & R. A. Gruendl, et al. 2006, ApJ, sub.

Reipurth, B., Bally, J., Fesen, R. A., & Devine D. 1998, Nature 396,343

This preprint was prepared with the AAS LaTeX macros v5.2.

Fig. 1.— Single-order echelle spectrograph of the jet system covering both H$\alpha$ and [NII]. The slit is oriented along the jet direction with a position angle of 315°. Upper panel: Wavelength calibrated single-order echelle spectrograph of the jet. Note that the jet is clearly resolved into two distinct velocity components as disclosed by especially the [NII] emission lines, which have a less thermal dispersion than H$\alpha$. Line emission from both the receding and the approaching shells of the HII region are well resolved and presented. Lower panel: Net emission from the jet system after careful background subtraction.

Fig. 2.— Position-Velocity diagrams of the H$\alpha$ (left panel) and [NII] $\lambda\lambda$6583 emission (right panel) from the jet system. The radial velocity in the abscissa is calibrated to the heliocentric rest frame. The ordinate indicates projected distance from the jet source, the position of which is marked as zero in the plot.

Fig. 3.— Normalized echelle spectrum of the jet-driving source (upper panel) and that of the jet (lower panel). Note about the double peak profiles associated with both of the [NII] emission lines. The intensity ratio of the two [NII] emission lines I($\lambda$6583)/I($\lambda$6548) in the source spectrum equals 3.6 and that in the jet 4.5. The equivalent width of H$\alpha$ emission of the jet at 10% intensity amounts to 163 Å, whilst that of the source spectrum is 5.8 Å.

Fig. 4.— Low-resolution spectrum of the jet source covering both H$\alpha$ and the [OIII] emission lines. Note about the red continuum of the energy source with a late spectral type.

Fig. 5.— Light variations of the jet source in both R (upper panel) and I (lower panel). Note about the detection of two flare-like events with a similar amplitude in both filters. The dot-dashed line in each panel indicates a fitted normal level of the brightness of the jet source with the large amplitude variations cancelled.

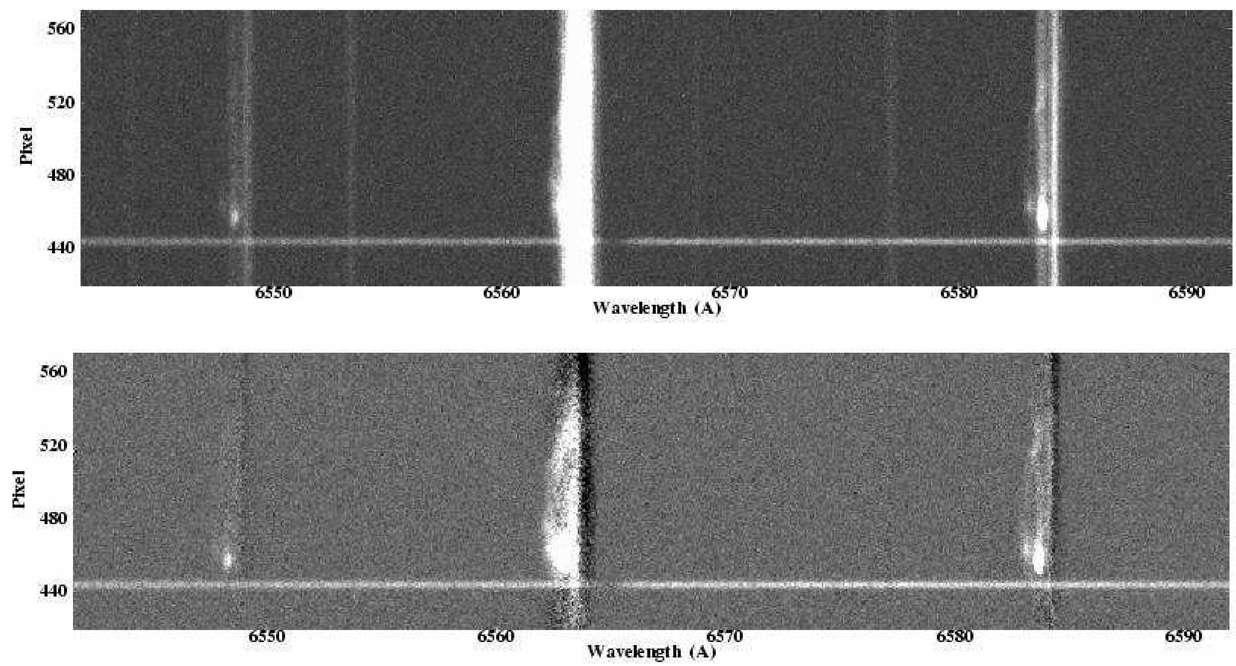
560
520
480
440
Pixel
6550
6560
6570
6580
6590
Wavelength (A)
560
520
480
440
Pixel
6550
6560
6570
6580
6590
Wavelength (A)

Fig.1

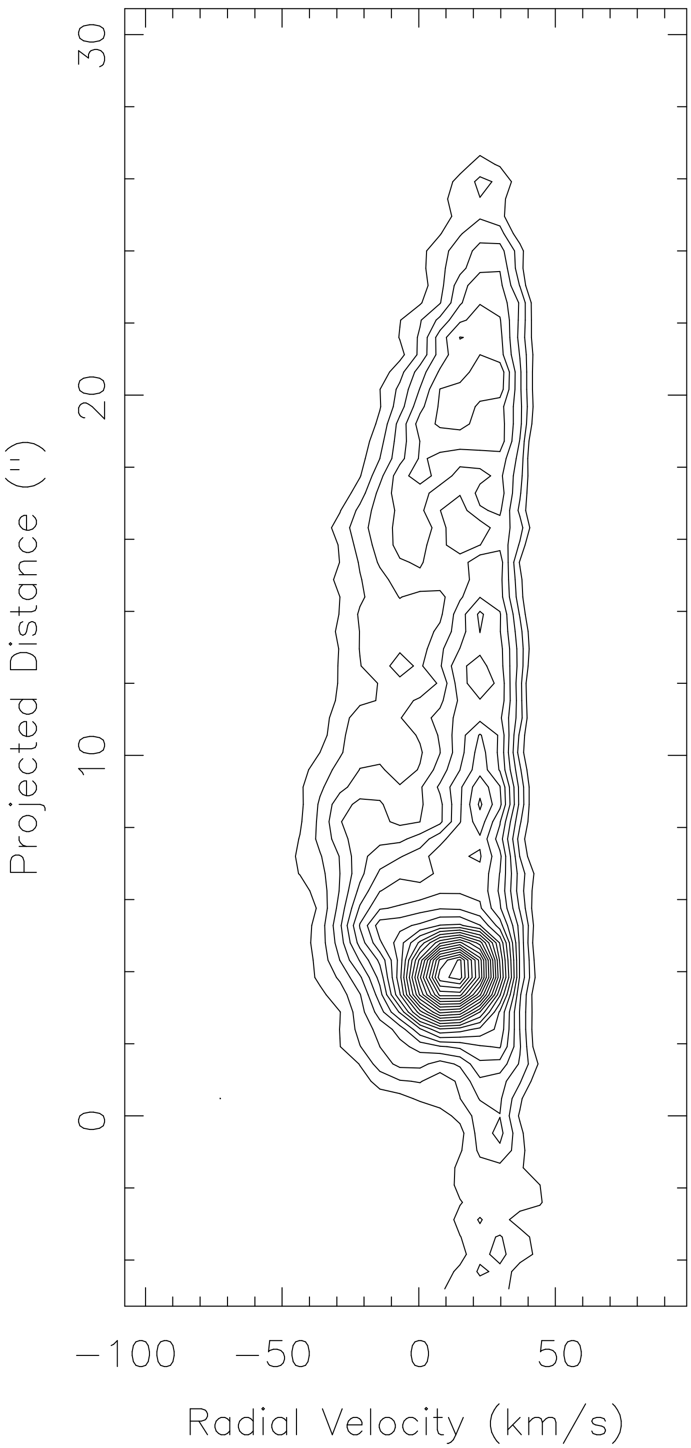
30
20
10
0
Projected Distance (")
−100
−50
0
50
Radial Velocity (km/s)

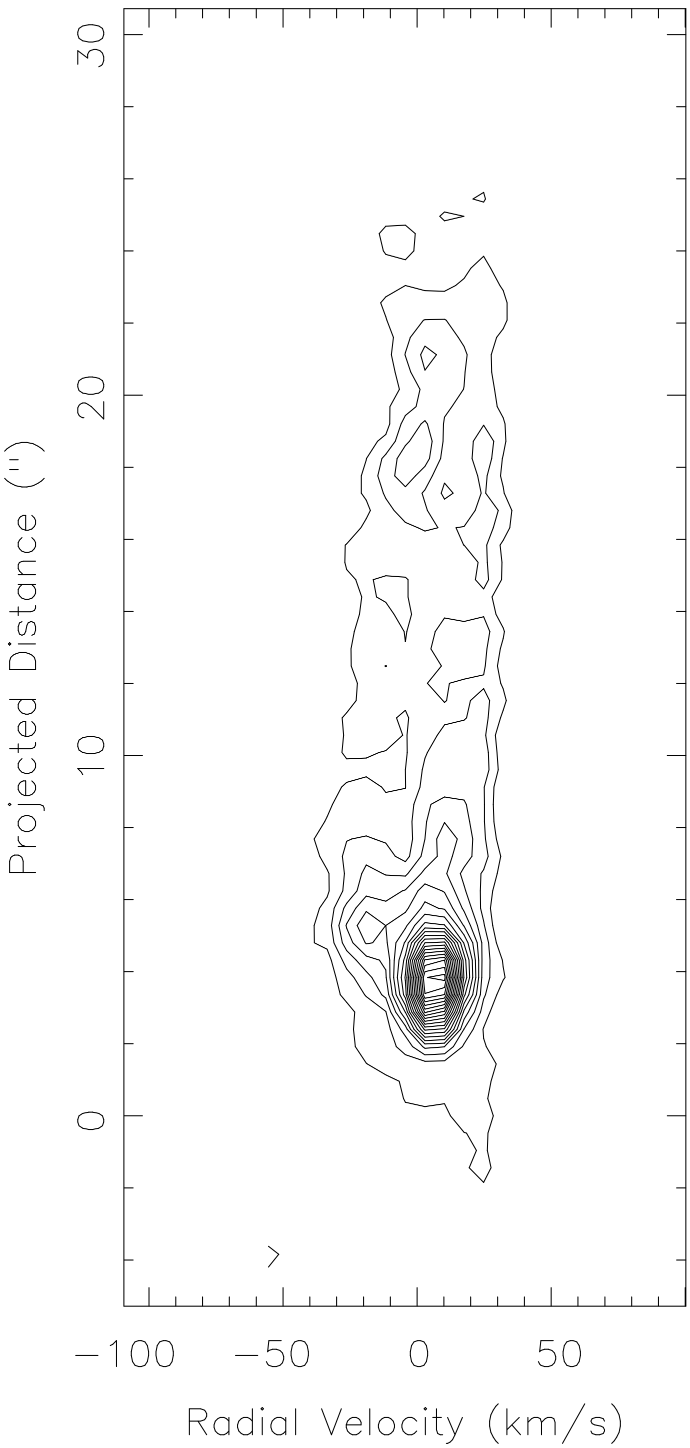


Fig.2

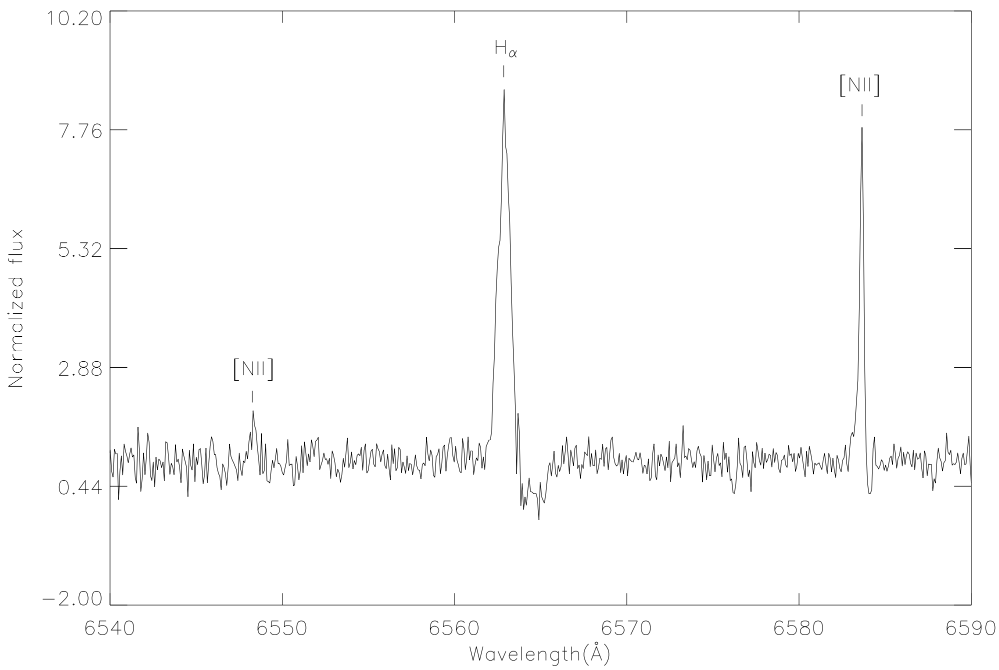
10.20
7.76
5.32
2.88
0.44
−2.00
Normalized flux
$H_\alpha$
[NII]
[NII]
6540
6550
6560
6570
6580
6590
Wavelength(Å)

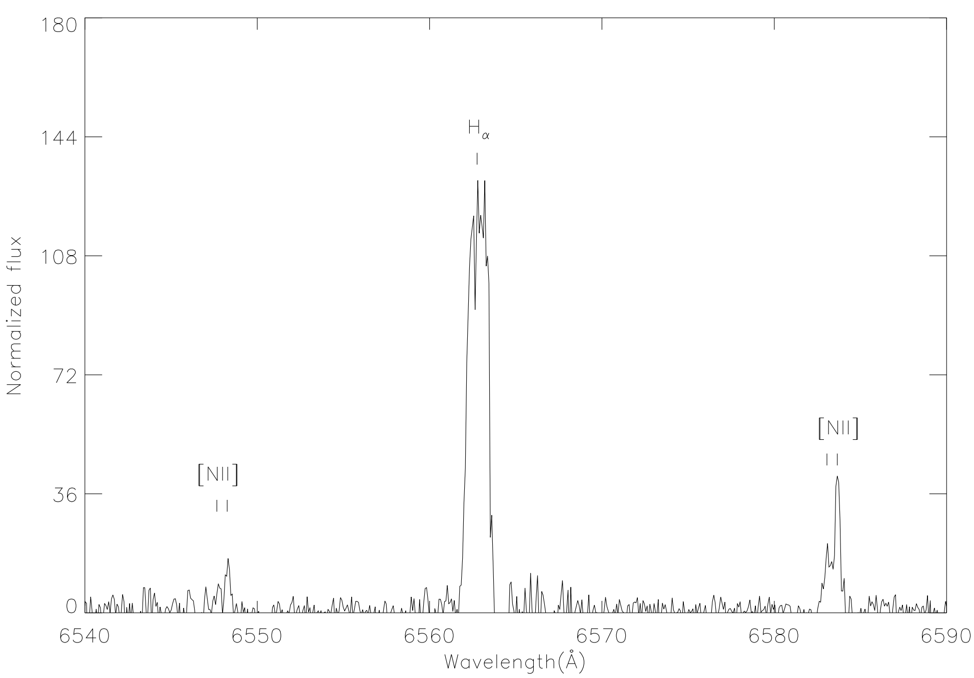
180
144
108
72
36
0
Normalized flux
$H_\alpha$
[NII]
[NII]
6540
6550
6560
6570
6580
6590
Wavelength(Å)

Fig.3

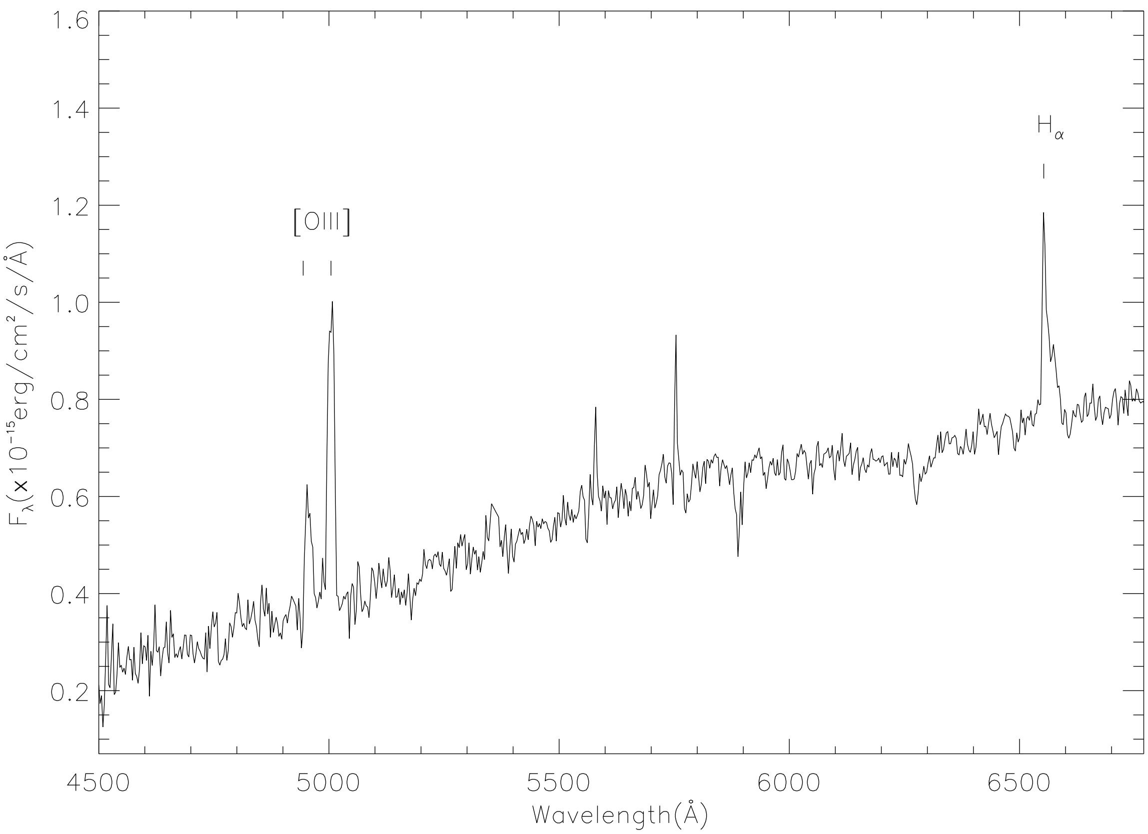
[OIII]
$H_\alpha$
$F_\lambda(\times10^{-15}erg/cm^2/s/Å)$
Wavelength(Å)
1.6
1.4
1.2
1.0
0.8
0.6
0.4
0.2
4500
5000
5500
6000
6500

Fig.4

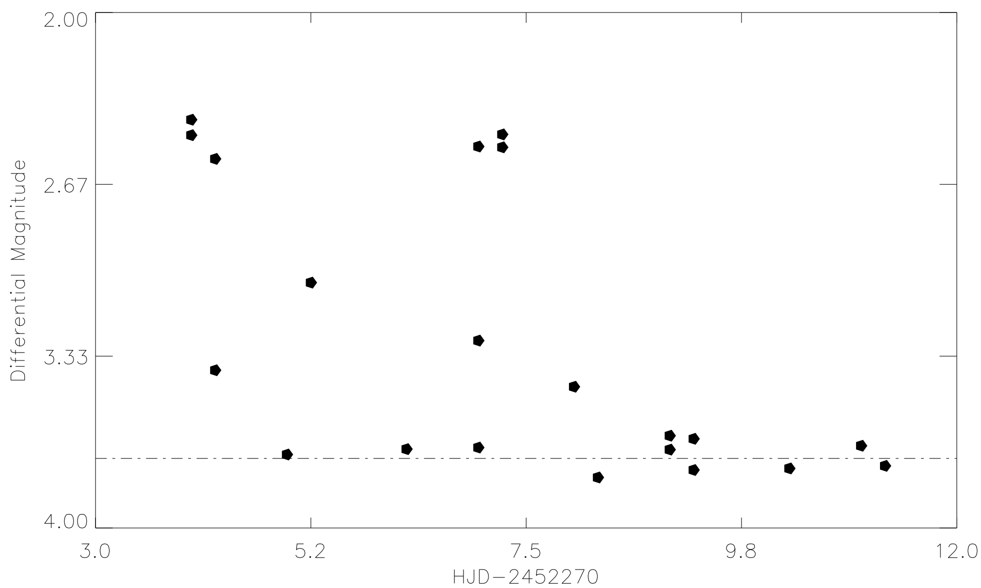
2.00
2.67
3.33
4.00
Differential Magnitude
3.0
5.2
7.5
9.8
12.0
HJD−2452270

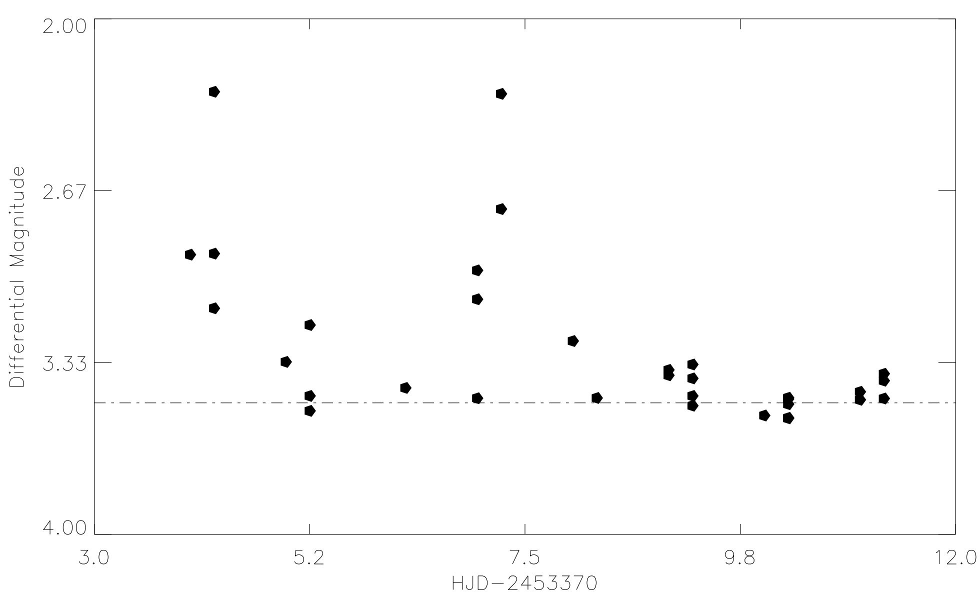
2.00
2.67
3.33
4.00
Differential Magnitude
3.0
5.2
7.5
9.8
12.0
HJD−2453370

Fig.5